2626 *Chem. Mater.* **2010,** *22,* 2626–2634
DOI:10.1021/cm9038076

CHEMISTRY OF MATERIALS
Article

Stimuli-Responsive Organosilica Hybrid Nanowires Decorated with Metal Nanoparticles

Jiayin Yuan,[†] Felix Schacher,[†] Markus Drechsler,[†] Andreas Hanisch,[†] Yan Lu,[‡] Matthias Ballauff,[‡] and Axel H. E. Müller*[,†]

[†]*Makromolekulare Chemie II, Universität Bayreuth, D-95440 Bayreuth, Germany, and* [‡]*Soft Matter and Functional Materials, Helmholtz−Zentrum Berlin für Materialien und Energie GmbH, 14109, Berlin, Germany*

Received December 18, 2009. Revised Manuscript Received February 22, 2010

We report on the synthesis and characterization of water-soluble stimuli-responsive organosilica hybrid nanowires that can be used as carriers for metallic nanoparticles. The nanowires were prepared from core−shell-structured cylindrical polymer brushes that served as templates with uniform size and shape. The core of the nanowires consists of a silsesquioxane network synthesized through a precursor route. The shell consists of a dense layer of poly(*N*,*N*-dimethylaminoethyl methacrylate) (PDMAEMA). The hybrid nanowires exhibit pH-responsive behavior, because of the weak polyelectrolyte nature of the PDMAEMA shell. Simultaneously, the shell of PDMAEMA acts as a nanoreactor for the synthesis and immobilization of metal nanoparticles. It was further quaternized with methyl iodide, leading to a poly{[2-(methacryloyloxy)ethyl] trimethylammonium iodide} (PMETAI) cationic polyelectrolyte shell around the silsesquioxane core. The as-synthesized cationic organosilica hybrid nanowires are sensitive to salt concentration, in terms of their hydrodynamic radius. They can be functionalized with platinum nanoparticles as well, leading to stable composites of the nanowires and the platinum nanoparticles. The nanocomposites show high catalytic activity, as kinetically analyzed in the reduction of 4-nitrophenol by sodium borohydride.

Introduction

The development of novel nanomaterials with advanced properties and improved performance is a continually expanding research area, which covers subjects ranging from chemistry, physics, biology, and medicine, to materials science. Apart from the inorganic counterpart, organic−inorganic hybrid nanomaterials have received considerable attention, because they not only represent a creative alternative to design new materials and compounds in academic activities, but their uncommon features allow the development of innovative industrial applications.[1−5] Among various systems, one-dimensional (1D) nanostructures such as nanowires, nanotubes, or nanorods have been the focus of recent research, because of their unusual size- and shape-dependent optical, electronic, and magnetic properties.[6−9] They have been used as building blocks and functional components in assembling nanodevices that can act as sensors, catalyst, lasers, waveguides, energy harvesters and generators.[8−14] Cylindrical polymer brushes (CPBs), that is, molecular brushes carrying linear or high-generation dendritic side chains densely grafted from a linear main chain, are suitable building blocks for 1D nanostructures.[15] The dense packing of side chains along the backbone leads to a stiffening of the main chain, which leads to the formation of unique structures in solution, in thin films, and in bulk.[16−18] Until now, various types of CPBs, differing in structure and chemical composition of

*Author to whom correspondence should be addressed. E-mail: axel.mueller@uni-bayreuth.de.

(1) Walther, A.; Yuan, J.; Abetz, V.; Müller, A. H. E. *Nano Lett.* **2009**, *9*(5), 2026–2030.
(2) Nicole, L.; Boissiere, C.; Grosso, D.; Quach, A.; Sanchez, C. *J. Mater. Chem.* **2005**, *15*(35−36), 3598–3627.
(3) Sanchez, C.; Boissiere, C.; Grosso, D.; Laberty, C.; Nicole, L. *Chem. Mater.* **2008**, *20*(3), 682–737.
(4) Sanchez, C.; Julian, B.; Belleville, P.; Popall, M. *J. Mater. Chem.* **2005**, *15*(35−36), 3559–3592.
(5) Sanchez, C.; de Soler-Illia, G. J.; Ribot, F.; Lalot, T.; Mayer, C. R.; Cabuil, V. *Chem. Mater.* **2001**, *13*(10), 3061–3083.
(6) Xia, Y.; Yang, P.; Sun, Y.; Wu, Y.; Mayers, B.; Gates, B.; Yin, Y.; Kim, F.; Yan, H. *Adv. Mater.* **2003**, *15*(5), 353–389.
(7) Ludovico, C.; Geoffrey, A. O. *Adv. Mater.* **2009**, *21*(9), 1013–1020.
(8) Duan, X.; Lieber, C. M. *Adv. Mater.* **2000**, *12*(4), 298–302.
(9) Greiner, A.; Wendorff, J. H. *Angew. Chem., Int. Ed.* **2007**, *46*(30), 5670–5703.
(10) Wang, Z. L.; Song, J. *Science* **2006**, *312*(5771), 242–246.
(11) Johnson, J. C.; Choi, H.-J.; Knutsen, K. P.; Schaller, R. D.; Yang, P.; Saykally, R. J. *Nat. Mater.* **2002**, *1*(2), 106–110.
(12) Dai, H.; Hafner, J. H.; Rinzler, A. G.; Colbert, D. T.; Smalley, R. E. *Nature* **1996**, *384*(6605), 147–150.
(13) Murphy, C. J.; Sau, T. K.; Gole, A. M.; Orendorff, C. J.; Gao, J.; Gou, L.; Hunyadi, S. E.; Li, T. *J. Phys. Chem. B* **2005**, *109*(29), 13857–13870.
(14) Huynh Wendy, U.; Dittmer Janke, J.; Alivisatos, A. P. *Science* **2002**, *295*(5564), 2425–7.
(15) Yuan, J.; Xu, Y.; Walther, A.; Bolisetty, S.; Schumacher, M.; Schmalz, H.; Ballauff, M.; Müller, A. H. E. *Nat. Mater.* **2008**, *7* (9), 718–722.
(16) Zhang, M.; Müller, A. H. E. *J. Polym. Sci., Part A: Polym. Chem.* **2005**, *43*(16), 3461–3481.
(17) Dziezok, P.; Sheiko, S. S.; Fischer, K.; Schmidt, M.; Möller, M. *Angew. Chem., Int. Ed.* **1998**, *36*(24), 2812–2815.
(18) Sheiko, S. S.; Sumerlin, B. S.; Matyjaszewski, K. *Prog. Polym. Sci.* **2008**, *33*(7), 759–785.

Published on Web 03/10/2010

the backbone, as well as the side chains, have been synthesized.[18] Among these systems, the core−shell-structured CPBs that carry diblock copolymer side chains are of particular interest.[19−25] A combination of incompatible blocks in the side chains may result in an intramolecular phase separation. This can create a 1D core surrounded by a protective shell. The anisotropic-shaped CPB core thus obtained can be practically used as a unimolecular template and nanoreactor for the synthesis of 1D inorganic or hybrid nanostructures.[15,26−30] Thus, metal precursors such as Cd^{2+}, Fe^{2+}/Fe^{3+}, $AuCl_4^-$, and Ti^{4+} ions could be immobilized within the linear core via complexation or transalcoholysis. In a subsequent step, chemical reactions, such as reduction or hydrolysis, were used to convert the precursors into corresponding nanoparticles (γ-Fe_2O_3,[26] CdS,[27] CdSe,[28] gold,[29] and TiO_2[30]) in the core.

Very recently, we have developed a different approach to template 1D organosilica, as well as inorganic silica nanowires, by CPB.[15] In this approach, the silica precursor was integrated into the monomer unit, which was then polymerized into the core block of the CPBs. Thus, the precursor acts as a building block of the CPB itself, instead of being externally introduced. Condensation of these moieties then leads to a silsesquioxane nanowire in each CPB core, which is solubilized by a poly(oligoethyleneglycol methacrylate) shell. Generally, these inorganic and hybrid 1D nanostructures templated by CPBs form stable colloidal solutions. In this strategy, which starts from a chemically bound precursor, the dimension of the resulting 1D nanostructure is strictly controlled by the CPB structure, the size and polydispersity of which are well-defined via the controlled polymerization technique.

Here, we take the next step by synthesizing core−shell nanowires that can be used as colloidal nanoreactors for the preparation and immobilization of metal nanoparticles. This goal is achieved by attaching a protective shell made up of *N*,*N*-dimethylaminoethyl methacrylate (DMAEMA) to the organosilica hybrid nanowires. The resulting core−shell nanowires with a poly(DMAEMA) (PDMAEMA) shell act as nanoreactors for the synthesis and immobilization of metal nanoparticles. Figure 1 shows the route employed here. First, we make use of atom transfer radical polymerization (ATRP) to graft PAPTS-*b*-PDMAEMA diblock copolymer side chains from a PBIEM polyinitiator backbone carrying 3200 ATRP initiating sites. 3-(Acryloylpropyl)trimethoxysilane (APTS) and DMAEMA monomers were sequentially polymerized using benzene as a solvent and CuBr/*N*,*N*,*N*′,*N*″,*N*″-pentamethyldiethylenetriamine (PMDETA) or HMDETA as the catalyst system. Ammonia-catalyzed condensation of the inner PAPTS block leads to a silsesquioxane network in the core. In this way, the core−shell CPB was converted to organosilica hybrid nanowires ($[(SiO_{1.5})_{72}$-*b*-$DMAEMA_{95}]_{3200}$) solubilized by a PDMAEMA shell, which is a weak polyelectrolyte. Quaternization of the PDMAEMA shell was achieved by reaction with methyl iodide, transferring the PDMAEMA shell into a strong cationic polyelectrolyte PMETAI. Both organosilica hybrid nanowires with either a PDMAEMA or PMETAI shell can be functionalized in a final step by metal nanoparticles (see Figure 1). The catalytic property of these composites was checked using a model reaction, and the catalytic activity was compared to data from previous literature.[31,32] Note that, in a different synthetic route, Sanchez et al. prepared various types of 1D inorganic−organic silica and other hybrid nanostructures. In their strategy, a "supramolecular assembly" concept was adopted through the employment of low-molecular-weight organogelators (LMOGs) as building blocks to construct the 1D hybrid nanostructures. The as-synthesized hybrids could be redispersed into water and further functionalized with metal nanoparticles.[33,34]

Experimental Section

Materials. All chemicals were of analytical grade and used as received without further purifications, except that 3-trimethoxysilylpropyl acrylate (APTS) (95%, ABCR) and *N*,*N*-dimethylaminoethyl methacrylate (98%, Aldrich) were filtered through an neutral alumina column shortly before each polymerization.

Preparation of Organosilica Hybrid Nanowires with a PDMAEMA Shell ($[(SiO_{1.5})_{72}$-*b*-$DMAEMA_{95}]_{3200}$). The polyinitiator backbone poly(2-bromoisobutyryloxyethyl methacrylate) (PBIEM) was prepared as reported earlier.[23] Its degree of polymerization (DP) and polydispersity index (PDI) was characterized to be 3200 and 1.14, respectively.[30] The synthetic procedure of PAPTS homopolymer CPB $[APTS_{72}]_{3200}$ was detailed in our previous paper.[15]

The atom transfer radical polymerization (ATRP) of DMAEMA as the outer shell block was conducted in benzene to suppress the hydrolysis and condensation of the trimethoxysilyl groups in the PAPTS shell block. The polymerization ran as follows: Into a flask equipped with a septum and magnetic

(19) Cheng, G.; Böker, A.; Zhang, M.; Krausch, G.; Müller, A. H. E. *Macromolecules* **2001**, *34*(20), 6883–6888.
(20) Ishizu, K.; Kakinuma, H. *J. Polym. Sci. Part A: Polym. Chem.* **2005**, *43*(1), 63–70.
(21) Boerner, H. G.; Beers, K.; Matyjaszewski, K.; Sheiko, S. S.; Moeller, M. *Macromolecules* **2001**, *34*(13), 4375–4383.
(22) Djalali, R.; Hugenberg, N.; Fischer, K.; Schmidt, M. *Macromol. Rapid Commun.* **1999**, *20*(8), 444–449.
(23) Zhang, M.; Breiner, T.; Mori, H.; Müller, A. H. E. *Polymer* **2003**, *44*(5), 1449–1458.
(24) Lee, H.; Jakubowski, W.; Matyjaszewski, K.; Yu, S.; Sheiko, S. S. *Macromolecules* **2006**, *39*(15), 4983–4989.
(25) Cheng, C.; Qi, K.; Khoshdel, E.; Wooley, K. L. *J. Am. Chem. Soc.* **2006**, *128*(21), 6808–6809.
(26) Zhang, M.; Estournes, C.; Bietsch, W.; Müller, A. H. E. *Adv. Funct. Mater.* **2004**, *14*(9), 871–882.
(27) Zhang, M.; Drechsler, M.; Müller, A. H. E. *Chem. Mater.* **2004**, *16*(3), 537–543.
(28) Yuan, J.; Drechsler, M.; Xu, Y.; Zhang, M.; Müller, A. H. E. *Polymer* **2008**, *49*(6), 1547–1554.
(29) Djalali, R.; Li, S.-Y.; Schmidt, M. *Macromolecules* **2002**, *35*(11), 4282–4288.
(30) Yuan, J.; Lu, Y.; Schacher, F.; Lunkenbein, T.; Weiss, S.; Schmalz, H.; Müller, A. H. E. *Chem. Mater.* **2009**, *21*(18), 4146–4154.
(31) Esumi, K.; Isono, R.; Yoshimura, T. *Langmuir* **2003**, *20*(1), 237–243.
(32) Mei, Y.; Sharma, G.; Lu, Y.; Ballauff, M.; Drechsler, M.; Irrgang, T.; Kempe, R. *Langmuir* **2005**, *21*(26), 12229–12234.
(33) Rambaud, F.; Valle, K.; Thibaud, S.; Julian-Lopez, B.; Sanchez, C. *Adv. Funct. Mater.* **2009**, *19*(18), 2896–2905.
(34) Llusar, M.; Sanchez, C. *Chem. Mater.* **2008**, *20*(3), 782–820.

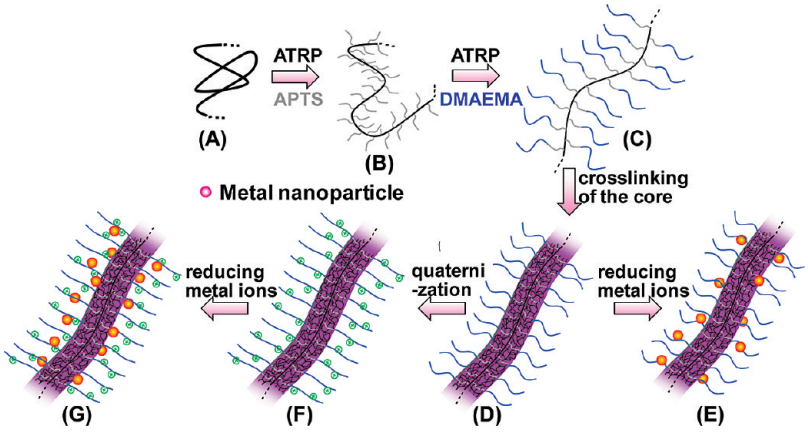

Figure 1. Synthesis of metal nanoparticle-functionalized organosilica hybrid nanowires templated by core−shell-structured CPBs: (A) ATRP polyinitiator backbone poly(2-bromoisobutyryloxyethyl methacrylate) (PBIEM) with DP ≈ 3200; (B) CPB with side chains of 72 APTS units; (C) core−shell CPB with an additional 95 DMAEMA units; (D) soluble organosilica hybrid nanowires with a cross-linked silsesquioxane network in the core and a weak polyelectrolyte PDMAEMA in the shell; (E) metal nanoparticle-functionalized organosilica hybrid nanowires ($[(SiO_{1.5})_{72}$-*b*-$DMAEMA_{95}]_{3200}$); (F) quaternized organosilica hybrid nanowires ($[(SiO_{1.5})_{72}$-*b*-$METAI_{95}]_{3200}$), and (G) the corresponding metal nanoparticle-functionalized products. See Figure 2 for the chemical structures.

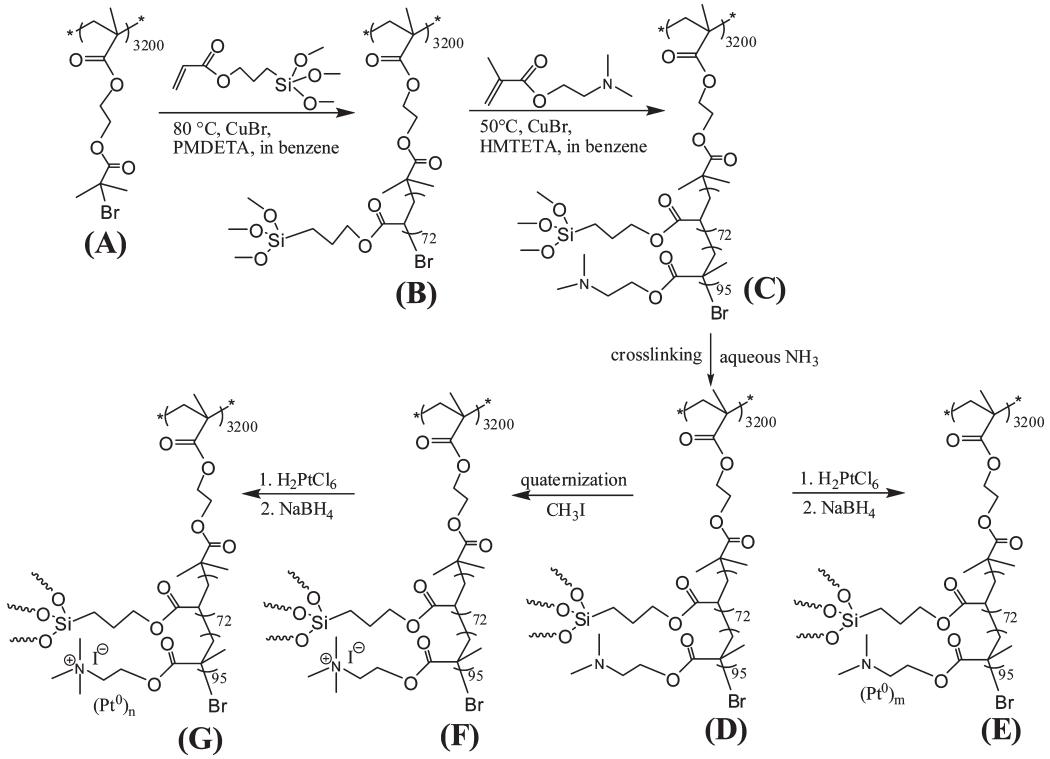

Figure 2. Synthetic route to metal nanoparticle-functionalized organosilica hybrid nanowires templated by core−shell-structured CPBs: (A) ATRP polyinitiator PBIEM; (B) $[APTS_{72}]_{3200}$ CPB; (C) $[APTS_{72}$-*b*-$DMAEMA_{95}]_{3200}$ core−shell CPB; (D) soluble $[(SiO_{1.5})_{72}$-*b*-$DMAEMA_{95}]_{3200}$ organosilica hybrid nanowires; (E) platinum-nanoparticle-functionalized $[(SiO_{1.5})_{72}$-*b*-$DMAEMA_{95}]_{3200}$; (F) cationic organosilica hybrid nanowires $[(SiO_{1.5})_{72}$-*b*-$METAI_{95}]_{3200}$; and (G) platinum-nanoparticle-functionalized $[(SiO_{1.5})_{72}$-*b*-$METAI_{95}]_{3200}$.

stirring bar, Cu(I)Br, PAPTS homopolymer CPB $[APTS_{72}]_{3200}$ (as a poly(macroinitiator)), DMAEMA, and benzene were loaded. The mixture was bubbled with argon for 30 min. An initial sample was taken for ^{1}H NMR measurement. The reaction bottle then was placed in a water bath at 50 °C. Finally, the degassed ligand 1,1,4,7,10,10-hexamethyltriethylenetetramine (HMTETA) was injected to start the polymerization. The polymerization was monitored by taking samples out of the reaction flask for ^{1}H NMR measurements. The polymerization was stopped by cooling the reaction mixture to room temperature and exposing it to air; the DP of the PDMAEMA block was determined to be 72 by ^{1}H NMR measurement. The reaction mixture was filtered through a neutral alumina column to remove the copper catalyst. The purification and condensation were conducted in one pot by ultrafiltrition using methanol, then methanol with 10 vol % of aqueous ammonia (10 wt %), and finally deionized water as eluents.

Preparation of Organosilica Hybrid Nanowires with a PMETAI Shell ($[(SiO_{1.5})_{72}$-*b*-$METAI_{95}]_{3200}$). To 200 mg of $[(SiO_{1.5})_{72}$-*b*-$DMAEMA_{95}]_{3200}$ hybrid nanowires in 20 mL of dioxane, 0.25 g of methyl iodide was added under stirring at room temperature. The solution became turbid after 15 min.

The stirring continued for 3 days; the reaction mixture was dialyzed first against methanol and then against deionized water for one week. A solid product was obtained as a white powder after freeze-drying.

Preparation of Platinum Nanoparticles Functionalized Hybrid Nanowires with a PDMAEMA or PMETAI Shell. To 4 mg of $[(SiO_{1.5})_{72}$-*b*-$DMAEMA_{95}]_{3200}$ or 6 mg of $[(SiO_{1.5})_{72}$-*b*-$METAI_{95}]_{3200}$ organosilica hybrid nanowires in 10 mL of water, 1 mL of $H_2PtCl_6 \cdot 6H_2O$ aqueous solution (2 g/L) was added dropwise under stirring. After 24 h, 5 mL of freshly prepared ice-cold $NaBH_4$ aqueous solution (1 g/L) was added by syringe pump within 30 min. After 5 h, the reaction mixture was purified by ultrafiltration to remove excessive reagents, as well as free platinum nanoparticles.

Catalytic Experiment of Platinum-Nanoparticle-Functionalized Hybrid Organosilica Hybrid Nanowires ($[(SiO_{1.5})_{72}$-*b*-$METAI_{95}]_{3200}$). A quantity of 0.5 mL of $NaBH_4$ solution (60 mmol/L) was added to 2.5 mL of 4-nitrophenol solution (0.12 mmol/L) that was contained in a glass vessel. Then, 0.05 mL of platinum-nanoparticle-doped hybrid nanowires ($[(SiO_{1.5})_{72}$-*b*-$METAI_{95}]_{3200}$) solution ([Pt] = 3.75×10^{-3} mmol/L) was added. Immediately after the addition of the composite particles, ultraviolet (UV) spectra of the sample were taken every 3 min in the range of 250−550 nm. The rate constant of the reaction was determined by measuring the change in intensity of the peak at 400 nm with time.

Characterization Methods. Transmission electron microscopy (TEM) images were taken on a Zeiss Model EM EF-TEM instrument operated at 200 kV. A 5 μL droplet of a dilute solution (0.02 g/L) in water was deposited onto a copper grid (200 mesh) that was coated with carbon film, followed by drying at room temperature for a short time. The statistical analysis of the size of nanowires and nanoparticles was performed using the UTHSCSA ImageTool program (University of Texas). In each case, 90−130 objects were measured to define the dimension.

Cryogenic transmission electron microscopy (cryo-TEM) was performed by drop-coating the dilute aqueous solution (0.02 g/L) on a hydrophilized lacey TEM grid, where most of the liquid was removed with blotting paper, leaving a thin film stretched over the grid holes. The specimens were shock-frozen by rapid immersion into liquid ethane and cooled to ~90 K by liquid nitrogen in a temperature-controlled freezing unit (Zeiss Cryobox, Zeiss NTS GmbH, Oberkochen, Germany). After the specimens were frozen, the remaining ethane was removed using blotting paper. The specimen was inserted into a cryo-transfer holder (Gatan Model CT3500, München, Germany) and transferred to a Zeiss Model EM922 EF-TEM instrument that was operated at 200 kV.

Scanning electron microscopy (SEM) and energy-dispersive X-ray (EDX) analysis was performed using a Zeiss Model 1530 Gemini instrument equipped with a field-emission cathode with a lateral resolution of ~2 nm. The samples were measured on silica wafer.

Dynamic light scattering (DLS) measurements were performed on a Model ALV DLS/SLS-SP 5022F compact goniometer system with a Model ALV 5000/E correlator and a He−Ne laser. CONTIN analyses were performed for the measured intensity correlation functions. The apparent hydrodynamic radii (R_h) were calculated using the Stokes−Einstein equation.

Thermogravimetric analysis (TGA) measurements were conducted on a Mettler Toledo Model TGA/SDTA 851 apparatus. The measurements were made under an airflow of 50 mL/min with heating from 30 °C to 700 °C (at a rate of 10 °C/min). Before TGA measurements, samples were collected from the brush solution by freeze-drying and dried in a vacuum oven at 50 °C for at least one day.

Proton nuclear magnetic resonance (^{1}H NMR) spectra were recorded to determine the monomer conversion and characterize the products on a Bruker Model AC-250 spectrometer at room temperature. Because of the limited concentration of organosilica hybrid nanowires, a large number of scan was used to enhance the signals in Figures 3C and 3D (presented later in this work).

Results and discussion

Synthesis of Brushes. The general synthetic route of the present research is schematically illustrated in Figure 1, whereas Figure 2 displays the details of the chemical structures. In our previous work, hybrid organosilica nanowires solubilized by a poly(oligoethyleneglycol methacrylate) (POEGMA) shell were templated from core−shell-structured CPBs.[15] The resultant nanowires are soluble in water, facilitating their further processing. However, the chemically inert POEGMA shell limits their application spectrum. In this paper, a versatile polymer poly(*N*,*N*-dimethylaminoethyl methacrylate) (PDMAEMA) was chosen as the nanowire shell, because of its multifunctionality, such as water solubility, pH responsiveness, ability to complex metal ions, and importantly, after quaternization creating cationic nanowires that are salt-sensitive and able to work as the catalyst carrier of metal nanoparticles.

A clear proof of the chemical structure is given by NMR spectroscopy. The protons in the PAPTS core and PDMAEMA shell have distinguishable chemical shifts and ^{1}H NMR spectra of the products at different steps were used to verify the success of the synthetic strategy. Figure 3A shows the ^{1}H NMR spectrum of the PBIEM polyinitiator backbone. When the PAPTS block side chain was grown directly from the polyinitiator backbone, peaks from the PBIEM backbone (peaks a, b, and c in Figure 3A) vanish, because of its rather low content (< 2%). New peaks that are characteristic of PAPTS appear in Figure 3B, i.e., the protons of the trimethoxysilyl groups (−Si(OCH_3)$_3$, indicated by intensive peak d, 3.5 ppm) and the methylene protons (−Si−CH_2−CH_2−CH_2−O, 4.1, 1.8, and 0.7 ppm). The $[APTS_{72}]_{3200}$ CPBs with ATRP initiating sites at the PAPTS chain ends then act as poly(macroinitiator)s for the side chain extension. After introducing the PDMAEMA shell block, followed by condensation of the PAPTS core, the trimethoxysilyl proton peak (peak d in Figure 3B) in the PAPTS block disappears, as a result of the condensation reaction. Through quaternization reaction with methyl iodide, the distinct peaks of dimethylaminoethyl groups in the PDMAEMA block (see peaks a, b, and c in Figure 3C) all shift to a higher region (see Figure 3D): methyl groups in the ammonium (peak c, 3.2 ppm), methylene groups adjacent to the ammonium (peak b, 3.8 ppm) and the other methylene groups to the ester groups (weak peak a, 4.5 ppm). Indeed, the quaternization reaction of the PDMAEMA block is quantitative, because no residual

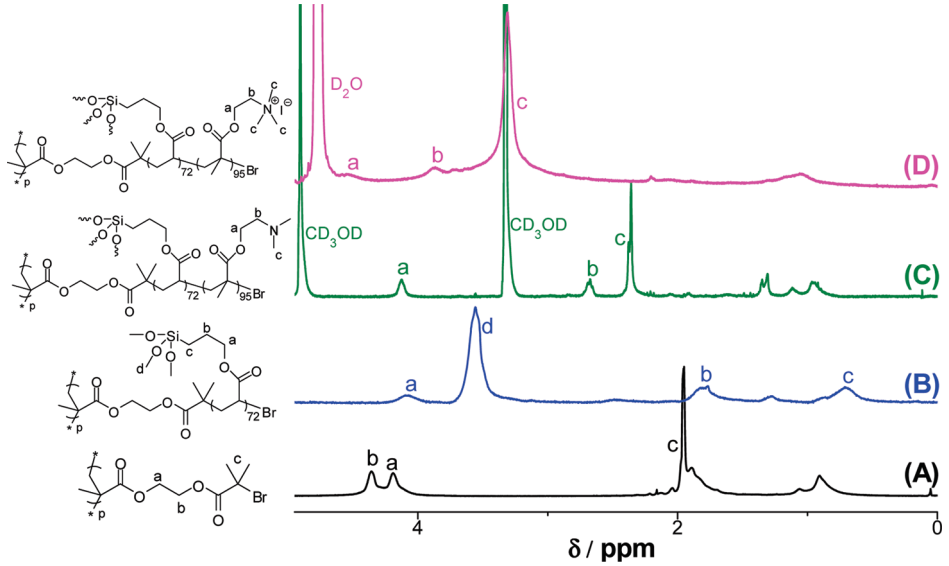

Figure 3. ^{1}H NMR spectra of (A) PBIEM polyinitiator backbone (in $CDCl_3$), (B) $[APTS_{72}]_{3200}$ CPB (C_6D_6), (C) $[(SiO_{1.5})_{72}$-*b*-$DMAEMA_{95}]_{3200}$ (in CD_3OD), and (D) $[(SiO_{1.5})_{72}$-*b*-$METAI_{95}]_{3200}$ (in D_2O) hybrid nanowires. The sharp peaks at 3.3 and 4.8 ppm in panel C, and 4.9 ppm in panel D, are from the residual NMR solvents (CD_3OD and D_2O, respectively).

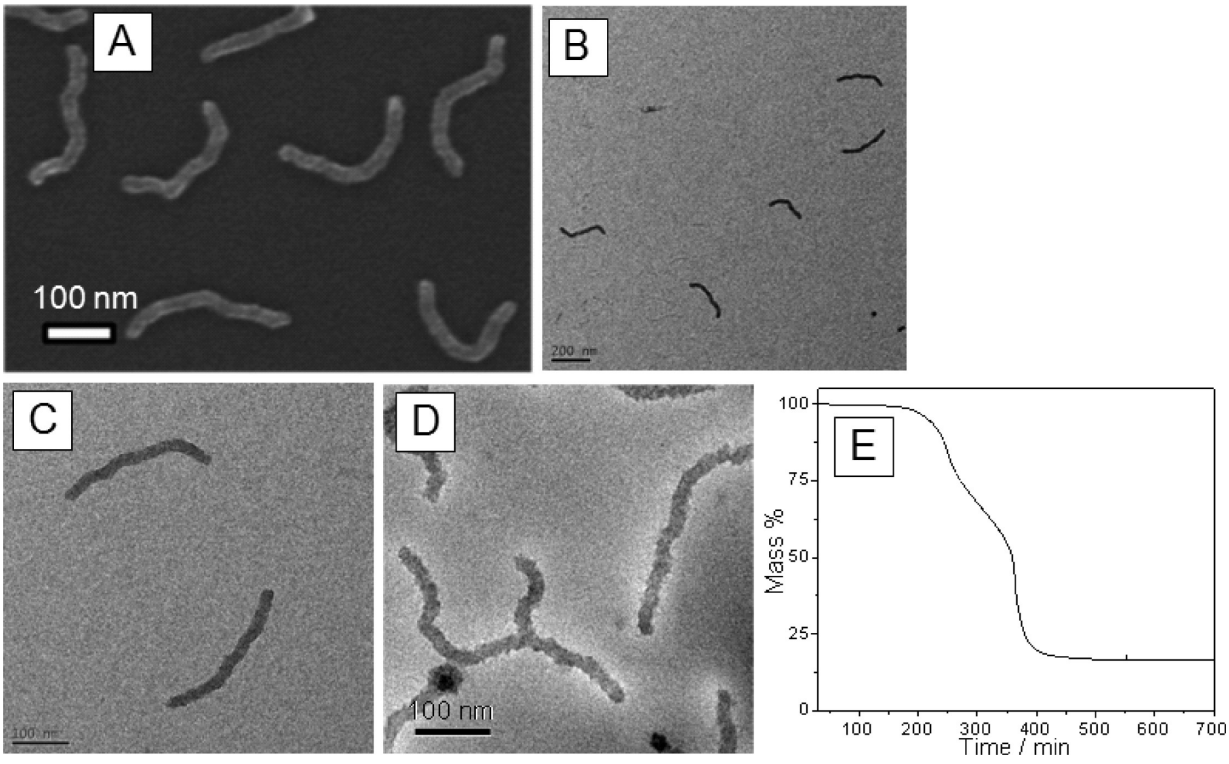

Figure 4. Characterization of organosilica hybrid nanowires with a PDMAEMA shell ($[(SiO_{1.5})_{72}$-*b*-$DMAEMA_{95}]_{3200}$): (A) SEM image on a silicon wafer; (B) TEM image; (C) its enlarged view; (D) cryo-TEM image; and (E) TGA curve.

peak was detected at the original positions (peaks a, b, and c in Figure 3C). Thus, the organosilica hybrid nanowires become positively charged, because of the cationic polyelectrolyte PMETAI shell.

Characterization of PDMAEMA Brushes. The prepared hybrid nanowires ($[(SiO_{1.5})_{72}$-*b*-$DMAEMA_{95}]_{3200}$) were visualized by scanning electron microscopy (SEM). As shown in Figure 4A, the wormlike morphology adopted on a silicon wafer is clearly visible, indicating the high stability of the polymeric cylinders during the polymerization and condensation process. The regular shape of these hybrid nanowires facilitates a statistical analysis, which shows that the average length is 270 ± 35 nm and the diameter is 31 ± 4 nm. This gives an aspect ratio of 9. In the SEM image, both the silsesquioxane core and the PDMAEMA shell are visible. Thus, the dimensions obtained above refer to the entire cylindrical structure. In the TEM characterization, the PDMAEMA shell is transparent, because of its rather low contrast, compared to the silsesquioxane core. Therefore, they

appear thinner. Figure 4B depicts a typical TEM image of the organosilica hybrid nanowires ($[(SiO_{1.5})_{72}$-*b*-$DMAEMA_{95}]_{3200}$) on a carbon-coated grid. The TEM micrographs demonstrate that these wires are evenly dispersed and are uniform in size. An enlarged view in Figure 4C clearly shows that the diameter is constant all along the silsesquioxane nanowire. Their number-average length is 262 ± 29 nm, which is close to the SEM value. It appears that they are quite short, with respect to the contour length (3200 × 0.25 nm = 800 nm), i.e., ca. 33%. This is attributed to the contraction during the condensation process. The diameter is 20 ± 3 nm, resulting an aspect ratio of 13 for the silsesquioxane core. The thickness of the collapsed PDMAEMA shell is calculated to be 5−6 nm in the dried state.

The structural information obtained from the SEM and TEM characterizations only describes the hybrid nanowires in a dried state; therefore, additional information about the morphology of these hybrid worms in solution has been obtained by cryo-TEM measurements. Figure 4D displays the resulting micrographs. The contrast of the PDMAEMA shell in water is so weak that the shell becomes practically invisible under these conditions. However, cryo-TEM corroborates the wormlike shape of these nanowires inferred from measurements in the dried state. The exact content of the silica in the hybrid is determined by TGA. After decomposition of the organic moiety at 700 °C, 15.74% is detected as residue, which is close to the calculated value of 16.13%.

PDMAEMA has a high affinity to transition metals, because the amino groups contained in each repeating unit are capable of complexing metal ions.[35,36] This complexation has been used to prepare metal nanoparticles within the PDMAEMA polymer matrix. In the present system, the PDMAEMA shell can act as a nanoreactor for the generation of metal nanoparticles surrounding the organosilica hybrid nanowires. Moreover, it stabilizes the entire composite in an efficient manner. Thus, platinum nanoparticles were generated in the hybrid nanowire. The platinum precursor H_2PtCl_6 was first mixed with the nanowire solution in water to achieve the complexation between the metal ions and the PDMAEMA shell. Freshly prepared $NaBH_4$ aqueous solution then was added to reduce the metal ions to metal atoms, which nucleate and grow into nanoparticles within the shell. The formation of nanoparticles results in an instant change in the solution color from yellow to brown. The successful incorporation of nanoparticles in the hybrid nanowires is confirmed by TEM investigation. Figure 5A shows a low-magnification TEM image of platinum-nanoparticle-functionalized hybrid nanowires ($[(SiO_{1.5})_{72}$-*b*-$DMAEMA_{95}]_{3200}$). As can be seen clearly, the hybrids are still well-dispersed in solution, despite the platinum nanoparticles loaded in the shell. Each of the cylindrical hybrids (see Figure 5B) carries 100−200 platinum nanoparticles homogeneously distributed along the cylinder. Their average size is 1.95 ± 0.39 nm.

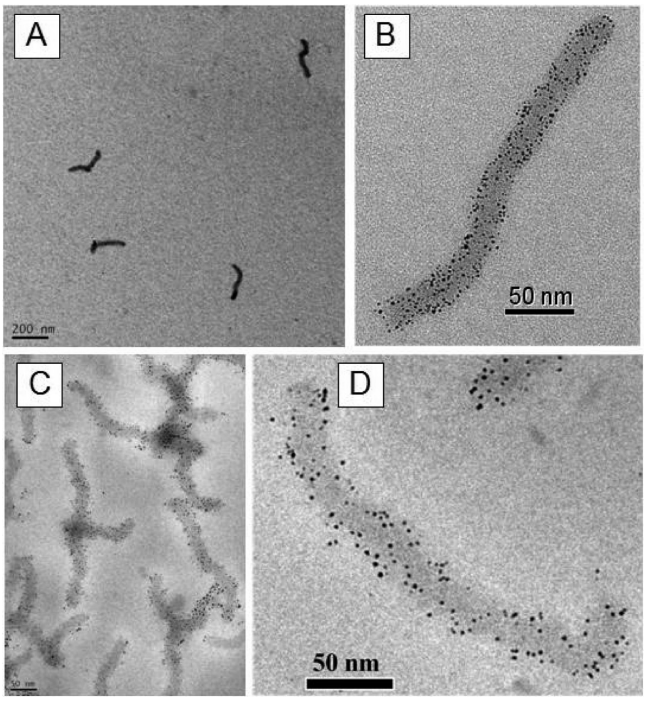

Figure 5. (A and B) TEM and (C and D) cryo-TEM images of platinum-functionalized organosilica hybrid nanowires ($[(SiO_{1.5})_{72}$-*b*-$DMAEMA_{95}]_{3200}$).

To exclude any drying effect related to the nanoparticles@nanowire morphology, cryo-TEM measurement of the aqueous sample is performed. As shown in Figure 5C and its enlarged view in Figure 5D, the platinum nanoparticles were solely generated on the surface of the worms. The density of the nanoparticle on the hybrid nanowires seems to be lower in the cryo-TEM measurement (Figure 5D) than that in the TEM image, Figure 5B. This is caused by the fact that cryo-TEM refers to the swollen state of the PDMAEMA shell, whereas Figure 5B shows the dried state. The amount of platinum is estimated from EDX analysis (see the Supporting Information). The Pt/Si atomic ratio determined via EDX is 0.17. Taking into account that the hybrid nanowires ($[(SiO_{1.5})_{72}$-*b*-$DMAEMA_{95}]_{3200}$) contain 15.74 wt % silica, the platinum content is determined to be 8 wt % in the hybrid. The molar ratio of Pt/amino groups is calculated to be 1/8. Thus, only a small fraction of the PDMAEMA chains is needed to bind the platinum, and the remaining free chains provide sufficient solubilization of the entire hybrids.

Being a weak polyelectrolyte, PDMAEMA can respond to a pH change in aqueous solution.[37−41] This

(35) Li, Z.; Sai, H.; Warren, S. C.; Kamperman, M.; Arora, H.; Gruner, S. M.; Wiesner, U. Chem. Mater. **2009**, *21* (23), 5578−5584.
(36) Zhang, M.; Liu, L.; Wu, C.; Fu, G.; Zhao, H.; He, B. *Polymer* **2007**, *48*(7), 1989–1997.
(37) Wang, M.; Zou, S.; Guerin, G.; Shen, L.; Deng, K.; Jones, M.; Walker, G. C.; Scholes, G. D.; Winnik, M. A. *Macromolecules* **2008**, *41*(19), 6993–7002.
(38) Ye, Q.; Wang, X.; Hu, H.; Wang, D.; Li, S.; Zhou, F. *J. Phys. Chem. C* **2009**, *113*(18), 7677–7683.
(39) Liu, Y.; Cao, X.; Luo, M.; Le, Z.; Xu, W. *J. Colloid Interface Sci.* **2009**, *329*(2), 244–252.
(40) Zhang, Y.; Gu, W.; Xu, H.; Liu, S. *J. Polym. Sci., Part A: Polym. Chem.* **2008**, *46*(7), 2379–2389.
(41) Xu, Y.; Bolisetty, S.; Drechsler, M.; Fang, B.; Yuan, J.; Ballauff, M.; Müller, A. H. E. *Polymer* **2008**, *49*, 3957–3964.

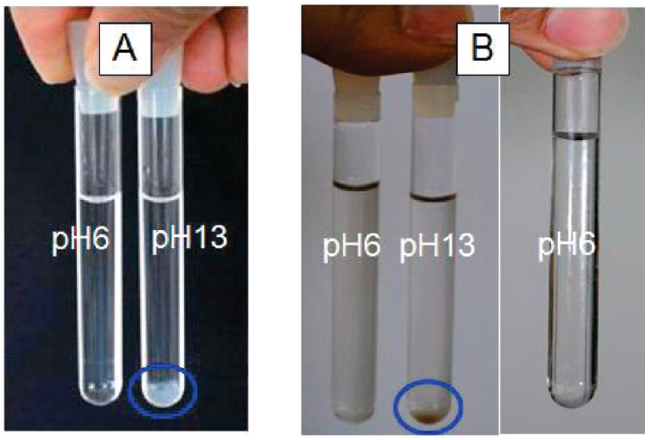

Figure 6. Photographs of pH-responsive behaviors of organosilica hybrid nanowires with a PDMAEMA shell (A) without and (B) with platinum nanoparticles in the shell. The concentrations of hybrid nanowires in both are 0.2 g/L.

allows us to manipulate the hybrid nanowires by changing the pH value of the solution. As shown in Figure 6, the hybrid nanowires in water (Figure 6A, left) appear as a stable dispersion (slightly scattering) at pH 6, (also when platinum (Figure 6B, left) nanoparticles were immobilized in the PDMAEMA shell). However, if the pH value increases to 13 by adding concentrated aqueous NaOH, flocculation results and white and brown precipitates were observed in both two vials (Figure 6A, right, and Figure 6B, middle). This instability is caused by the deprotonation of the amino groups in the PDMAEMA shell at high pH. Under these conditions, PDMAEMA is no longer soluble in water and the nanowires precipitate. However, after removing the supernatant and redissolving the precipitate at pH 6, a stable solution of platinum-nanoparticle-functionalized hybrid nanowires could be readily achieved (Figure 6B, right). In contrast, the nanoparticle-free organosilica hybrid nanowires failed to redissolve. Only small flocks were observed, even after ultrasonic treatment. This unusual nanoparticle-related stabilization effect of hybrid nanowires may be explained by two facts:

(1) At high pH, the PDMAEMA chains collapse and the silsesquioxane cores in different nanowires may contact each other, which eventually causes an internanowire cross-linking through further condensation. The nanoparticles thicken the PDMAEMA protective shell, sufficiently screening the silsesquioxane cores.

(2) As reported earlier, the side chains collapse into a pearl-necklace structure in a poor solvent.[16,42] The inhomogeneous collapse of side chains leaves part of the core surface area uncovered, enhancing the risk of cross-linking. In the presence of evenly distributed nanoparticles, the collapse of the shell seems to be more homogeneous. However, more studies are needed to clarify this finding entirely.

Characterization of PMETAI Brushes. In the following, the PDMAEMA shell in the hybrid nanowires ($[(SiO_{1.5})_{72}$-*b*-$DMAEMA_{95}]_{3200}$) were converted to a strong polyelectrolyte, poly{[2-(methacryloyloxy)ethyl] trimethylammonium iodide} (PMETAI) by quaternization.[43,44] Consequently, the resulting CPB carry cationic PMETAI side chains that exert a mutual Coulombic repulsion. However, the size of the hybrid nanowires, as obtained from SEM and TEM analyses, remains the same, because the silsesquioxane network in the core already leads to a fully rigid main chain. Figure 7A shows the SEM image of the quaternized hybrid nanowires ($[(SiO_{1.5})_{72}$-*b*-$METAI_{95}]_{3200}$) on a silica wafer. The high uniformity in the size can be seen directly. The analysis indicates that they are 275 ± 30 nm long and 30 ± 3 nm wide (on average). The TEM characterization in Figures 7B and 7C suggests that they have a length of 264 ± 25 nm and a diameter of 21 ± 4 nm. The wormlike morphology in water is confirmed by the cryo-TEM image shown in Figure 7D. The silica content is measured to be 11.11% (Figure 7E), in good agreement with the calculated value (namely, 10.73%).

In the absence of external salts, the majority of counterions are confined within the shell.[45,46] When salt is added, it screens the electrostatic interaction within the polyelectrolyte. The repulsion among the polyelectrolyte side chains is thus diminished and the chains adopt a more-coiled configuration. This lowers the overall hydrodynamic radius of hybrid nanowires in solution. Figure 8 shows the apparent hydrodynamic radii (R_h) of the hybrid nanowires ($[(SiO_{1.5})_{72}$-*b*-$METAI_{95}]_{3200}$), as a function of the NaBr concentration. All CONTIN plots show unimodal distributions of R_h with an increase in the polydispersity index from 0.16 to 0.25. In the absence of salt, the R_h value of the hybrid nanowires is 168 nm. Increasing the NaBr concentration from 0 M to 1 M leads to a decrease in R_h by 39 nm, which is 23% of the apparent hydrodynamic radius of the hybrid nanowire in a salt-free solution. When the salt concentration exceeds 1 M, a re-expansion in the hydrodynamic radii occurs. As reported previously,[41,47] Br^- ions have specific interactions with cationic polyelectrolyte chains that lead to a salting-in of the nanowires.[48] A higher NaBr concentration will prompt an adsorption of Br^- ions onto the polyelectrolyte chains, which is followed by a reswelling of the chains.

After quaternization, the cationic PMETAI side chains electrostatically interact with metal ions, which can be applied to generate and immobilize nanoparticles as well.[38,49] Using the procedure described previously, we generated platinum nanoparticles on the cationic organosilica hybrid nanowires via the reduction of H_2PtCl_6 by

(42) Polotsky, A.; Charlaganov, M.; Xu, Y.; Leermakers, F. A. M.; Daoud, M.; Müller, A. H. E.; Dotera, T.; Borisov, O. *Macromolecules* **2008**, *41*(11), 4020–4028.
(43) Xu, Y.; Bolisetty, S.; Drechsler, M.; Fang, B.; Yuan, J.; Harnau, L.; Ballauff, M.; Müller, A. H. E. *Soft Matter* **2009**, *5*(379), 379–384.
(44) Plamper, F. A.; Schmalz, A.; Penott-Chang, E.; Drechsler, M.; Jusufi, A.; Ballauff, M.; Müller, A. H. E. *Macromolecules* **2007**, *40* (16), 5689–5697.
(45) Pincus, P. *Macromolecules* **2002**, *24*(10), 2912–2919.
(46) Jusufi, A.; Likos, C. N.; Löven, H. *Phys. Rev. Lett.* **2001**, *88*(1), 018301.
(47) Ballauff, M. *Prog. Polym. Sci.* **2007**, *32*(10), 1135–1151.
(48) Mei, Y.; Ballauff, M. *Eur. Phys. J.* **2005**, *16*(3), 341–349.
(49) Li, W.; Gao, C.; Qian, H.; Ren, J.; Yan, D. *J. Mater. Chem.* **2006**, *16*, 1852–1859.

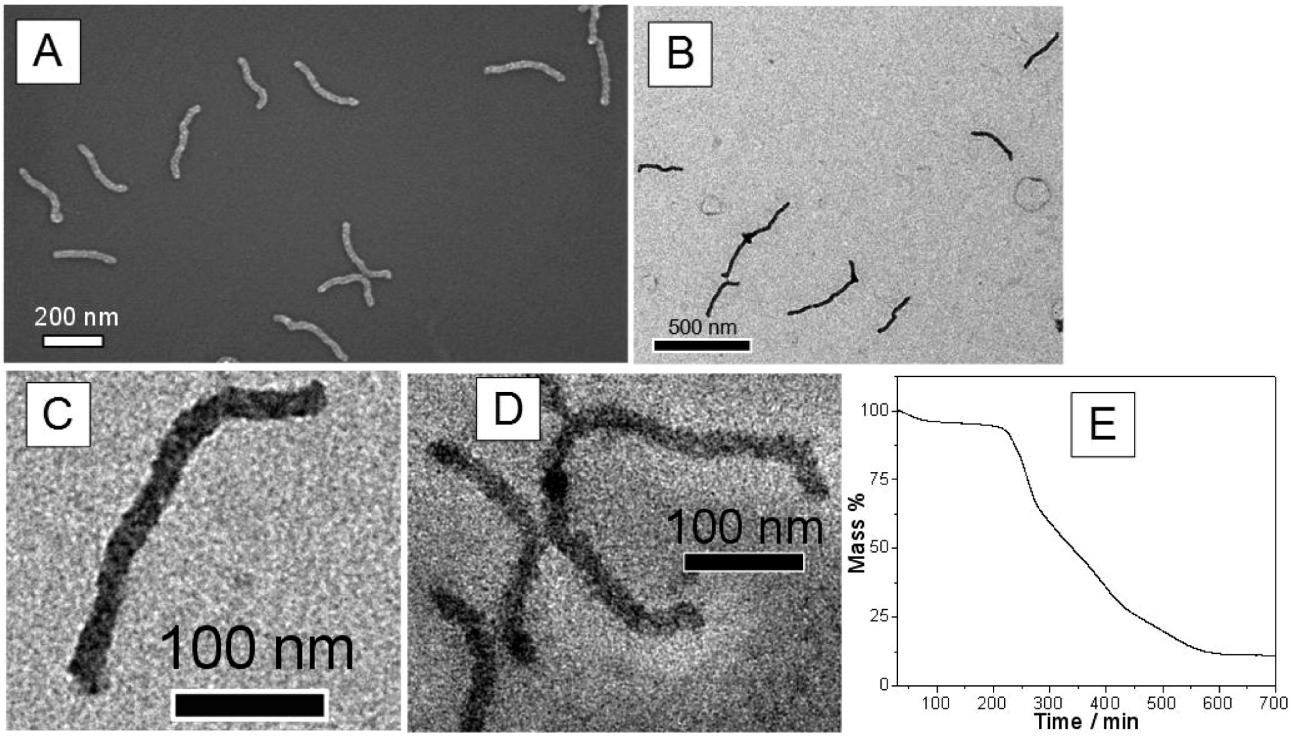

Figure 7. Characterization of organosilica hybrid nanowires with a PMETAI cationic polyelectrolyte shell ($[(SiO_{1.5})_{72}$-*b*-$METAI_{95}]_{3200}$): (A) SEM image on a silica wafer; (B) TEM image; (C) enlarged view of a nanowire (such as that shown in panel B); (D) cryo-TEM image; and (E) plotted TGA curve.

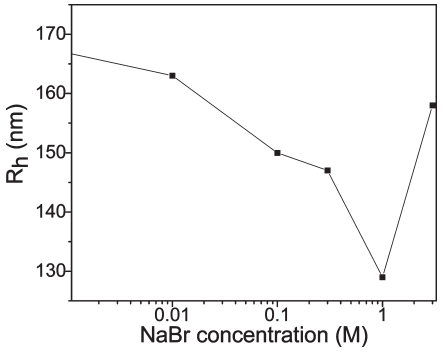

Figure 8. Apparent hydrodynamic radii of organosilica hybrid nanowires ($[(SiO_{1.5})_{72}$-*b*-$METAI_{95}]_{3200}$) with a PMETAI cationic shell (0.1 g/L) in aqueous solution at different NaBr concentrations.

$NaBH_4$. Figure 9A shows a TEM image of platinum-nanoparticle-decorated hybrid nanowires ($[(SiO_{1.5})_{72}$-*b*-$METAI_{95}]_{3200}$). The cryo-TEM image in Figure 9C proves that nanoparticles have formed exclusively on the hybrid nanowires. All hybrid nanowires were determined to be well-dispersed, and each worm carries approximately the same number of nanoparticles. In the enlarged view in Figure 9B, the nanoparticles on the nanowire appear different from that in Figure 5B, very probably due to the electrostatic interaction between the cationic PMETAI chains and the negatively charged platinum nanoparticles.[50] The nanoparticles are small and uniform in size (3.02 ± 0.51 nm). EDX analysis (see the Supporting Information) leads to a Pt/Si atomic ratio of 0.30, indicating that the platinum content is 75% higher than that in the $[(SiO_{1.5})_{72}$-*b*-$DMAEMA_{95}]_{3200}$ nanowires. The platinum content is determined to be 10 wt % of the entire hybrid.

To test the catalytic activity of the platinum nanoparticles, we performed the reduction of 4-nitrophenol by $NaBH_4$ in the presence of the platinum-nanoparticle-functionalized hybrid nanowires ($[(SiO_{1.5})_{72}$-*b*-$METAI_{95}]_{3200}$). This reaction has been used recently by several authors and has become a model reaction for testing the catalytic activity of nanoparticles.[31,32,51−59] As shown in Figure 9D, the strong UV absorption of 4-nitrophenate ions at 400 nm decreases gradually with time after the addition of platinum-nanoparticle-containing hybrid nanowires; simultaneously, a new peak appears at 300 nm, which is due to the product 4-aminophenol.[31,32] In addition, the concentration of sodium borohydride was adjusted to largely exceed the concentration of 4-nitrophenol. Therefore, in this case, pseudo-first-order kinetics, with regard to the 4-nitrophenol concentrations, could be used to evaluate the catalytic rate.[51] As shown in the inset of Figure 9D, a linear relationship between

(50) Lu, Y.; Mei, Y.; Walker, R.; Ballauff, M.; Drechsler, M. *Polymer* **2006**, *47*(14), 4985–4995.
(51) Pradhan, N.; Pal, A.; Pal, T. *Colloids Surf. A* **2002**, *196*, 247–257.
(52) Mei, Y.; Lu, Y.; Polzer, F.; Ballauff, M.; Drechsler, M. *Chem. Mater.* **2007**, *19*(5), 1062–1069.
(53) Lu, Y.; Mei, Y.; Schrinner, M.; Ballauff, M.; Moller, M. W.; Breu, J. *J. Phys. Chem. C* **2007**, *111*(21), 7676–7681.
(54) Panigrahi, S.; Basu, S.; Praharaj, S.; Pande, S.; Jana, S.; Pal, A.; Ghosh, S. K.; Pal, T. *J. Phys. Chem. C* **2007**, *111*(12), 4596–4605.
(55) Zhang, Q.; Zhang, T.; Ge, J.; Yin, Y. *Nano Lett.* **2008**, *8*(9), 2867–2871.
(56) Urs Peter, S. *Angew. Chem., Int. Ed.* **1975**, *14*(10), 679–688.
(57) Md. Harunar, R.; Tarun, K. M. *Adv. Funct. Mater.* **2008**, *18*(15), 2261–2271.
(58) Khalavka, Y.; Becker, J.; Sönnichsen, C. *J. Am. Chem. Soc.* **2009**, *131*(5), 1871–1875.
(59) Lee, J.; Park, J. C.; Song, H. *Adv. Mater.* **2008**, *20*(8), 1523–1528.

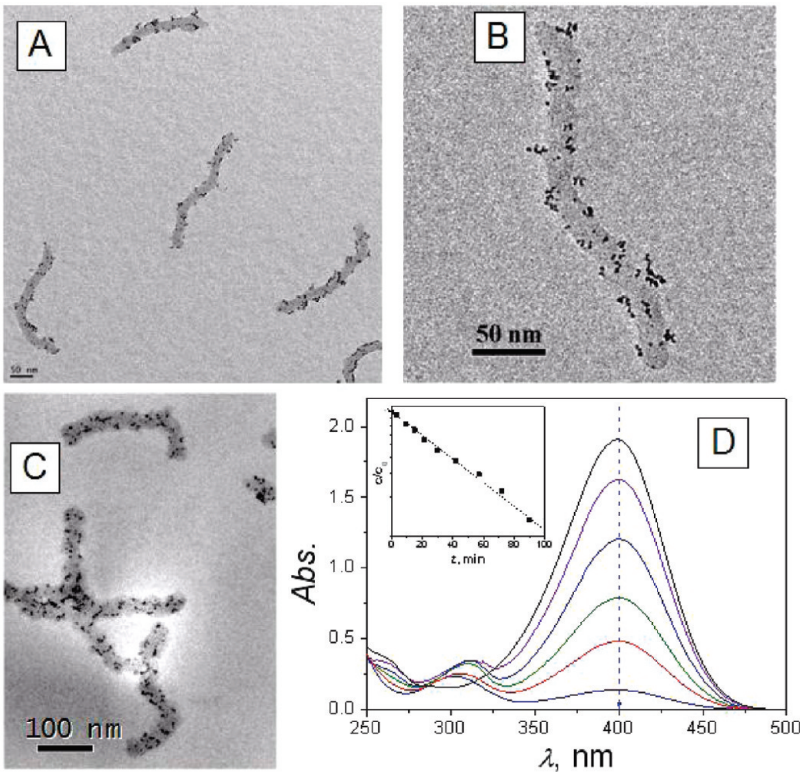

Figure 9. (A and B) TEM images and (C) cryo-TEm images of platinum-functionalized organosilica hybrid nanowires ($[(SiO_{1.5})_{72}$-b-$METAI_{95}]_{3200}$). (D) UV−vis kinetic curves of 4-nitrophenol during the reduction catalyzed by platinum-functionalized organosilica hybrid nanowires (inset shows a first-order plot).

$\ln(c_t/c_0)$ versus time t is obtained, from which the apparent rate constant ($k_{app} = 0.02\ min^{-1}$) is calculated.[52] Furthermore, k_{app} is proportional to the total surface area (S) of the metal nanoparticles present in the system:[53]

$$-\frac{dc_t}{dt} = k_{app}c_t = k_1 S c_t \qquad (1)$$

where c_t is the concentration of 4-nitrophenol at time t, k_1 is the rate constant normalized to S, which is the surface area of platinum nanoparticles ($d = 3$ nm, $A = 28\ nm^2$ per particle) normalized to the unit volume of the system. Using the bulk density of platinum ($\rho = 21.46 \times 10^3\ kg/m^3$), $k_1 = 0.31\ s^{-1}\,m^{-2}\,L$ is obtained, which is higher than that of platinum nanoparticles immobilized in dendrimers ($k_1 = 0.16\ s^{-1}\,m^{-2}\,L$)[26] and slightly lower than that measured for platinum nanoparticles immobilized in spherical polyelectrolyte brushes ($k_1 = 0.5\ s^{-1}\,m^{-2}\,L$).[27] This demonstrates that platinum-nanoparticle-functionalized hybrid nanowires can work as a stable catalyst carrier system in solution. Considering that the side chain of hybrid nanowires ($[(SiO_{1.5})_{72}$-*b*-$METAI_{95}]_{3200}$) is similar to that of cationic polyelectrolyte brushes, the difference of the catalytic activity of platinum nanoparticles is probably due to the relative larger size of the platinum nanoparticles ($d_{Pt} \approx 3$ nm), compared to that of spherical polyelectrolyte brush−Pt nanocomposites ($d_{Pt} \approx 2.1$ nm).

Conclusions

We prepared and characterized water-soluble organosilica hybrid nanowires that possess a poly(*N*,*N*-dimethylaminoethyl methacrylate) (PDMAEMA) weak polyelectrolyte shell templated from core−shell-structured cylindrical polymer brushes. The as-synthesized hybrid nanowires are uniform in size and act as nanoreactors for the synthesis and immobilization of metal nanoparticles. They show pH-responsive behavior, because of the weak polyelectrolyte nature of the PDMAEMA shell. In a following step, the shell of PDMAEMA was quaternized with methyl iodide, creating a poly{[2-(methacryloyloxy)ethyl] trimethylammonium iodide} (PMETAI) cationic polyelectrolyte shell around the silsesquioxane core. The cationic organosilica hybrid nanowires are salt-sensitive in aqueous solution, as detected by the change of their hydrodynamic radius. The nanowires were decorated using platinum nanoparticles. The catalytic activity of the resulting nanocomposites was proven in the reduction reaction of 4-nitrophenol by sodium borohydride. The excellent colloidal stability of the composite particles suggests the application as stable carrier system for catalysts. Work along these lines is underway.

Acknowledgment. This work was supported by the Deutsche Forschungsgemeinschaft (SPP 1165, Grant No. Mu896/22). We thank C. Löffler for help in TGA measurements. We appreciate valuable discussions with Dr. O. Borisov (Université de Pau, France).

Supporting Information Available: EDX spectra of platinum nanoparticle−functionalized organo-silica hybrid nanowires. This material is available free of charge via the Internet at http://pubs.acs.org.